Atomic Many-Body Effects in Neutrinos and Dark Matters Detection

Chih-Pan Wu

Dept. of Physics, National Taiwan University

Collaborators:

J.-W. Chen (National Taiwan University)
H.-C. Chi, C.-P. Liu (National Dong Hua University)
Henry T. Wong (Academia Sinica, TEXONO Collaboration)

Detectors with Pure Atoms

TEXONO HPGe Detector

The LZ Detector

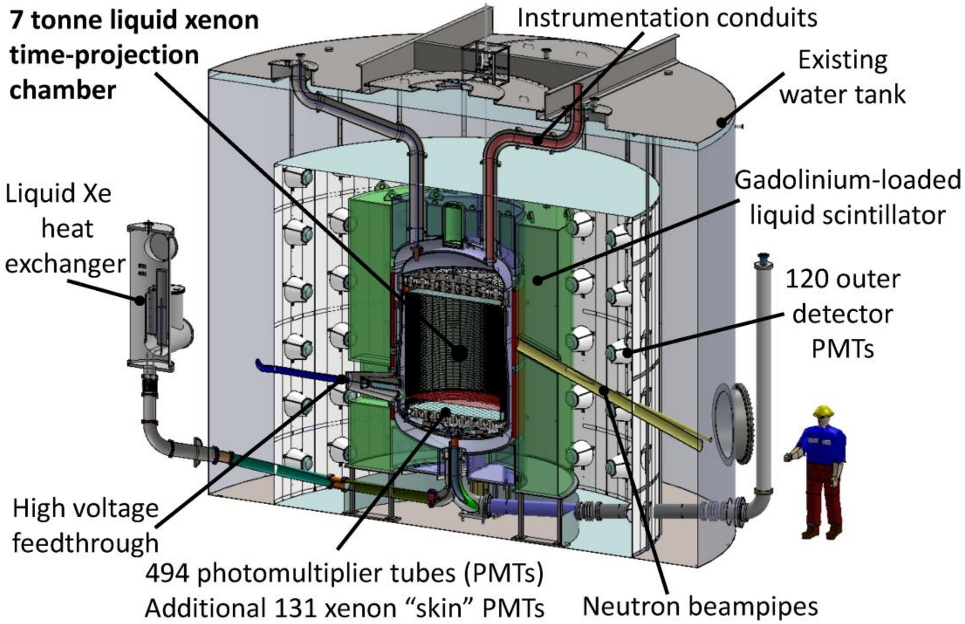

Lakhwinder Singh (25 Jul 2017, 17:15)

- Good energy resolution
- Lower analyzable recoil energy

- Very large fiducial mass
- Good NR/ER discrimination

Why we study atomic structure ?

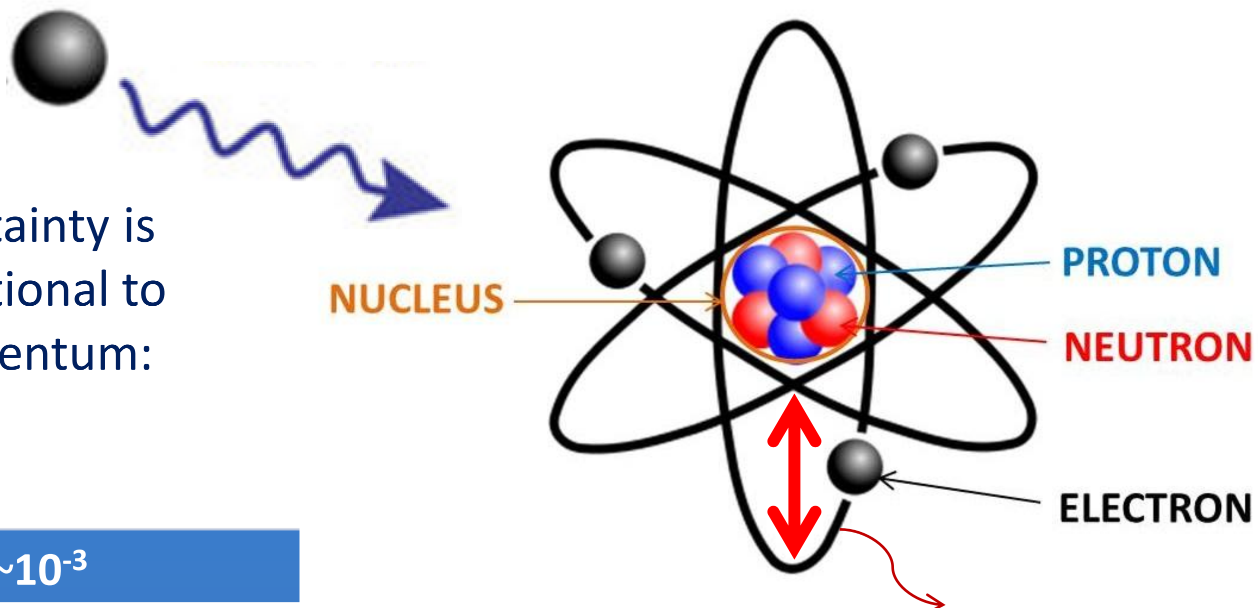

The space uncertainty is inversely proportional to its incident momentum:

$\lambda \sim 1/p$

Atomic Size is inversely proportional to its orbital momentum:

$Z m_e \alpha \sim Z$*3.7 keV

Z: effective charge

LDM with velocity ~10^{-3}		
Mass	Energy	Momentum
1 GeV	m_χ + 500 eV	1 MeV
100 MeV	m_χ + 50 eV	100 keV
Neutrino Sources		
Reactor ν	~ few MeV	Same as energy
Solar ν (pp)	~ few hundred keV	Same as energy

Scatter off: Free Target v.s. Atom

$$q^2 = -2\, m_e\, T$$

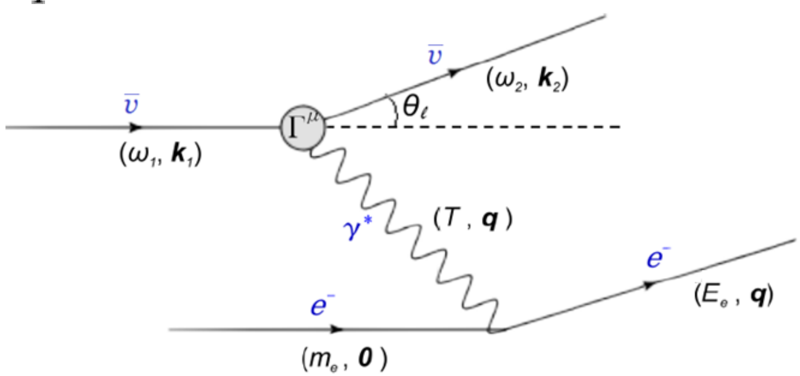

$$\nu + A \rightarrow \nu' + A^+ + e^-$$

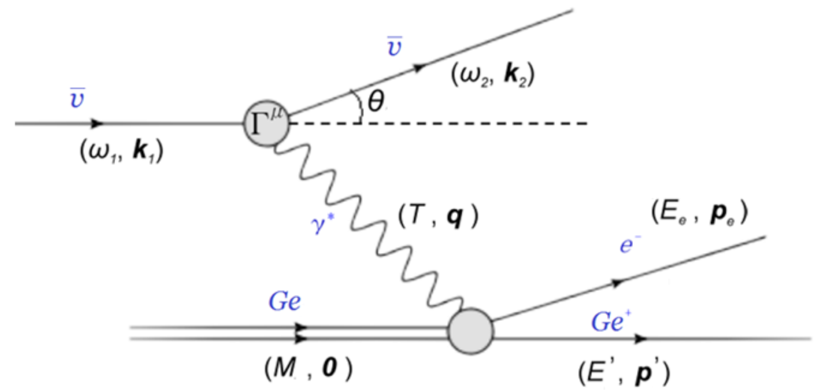

Phase space is fixed in 2-body scattering
→ 4-momentum transfer is fixed
→ scattering angle is fixed
→ Maximum energy transfer is limited

by a factor $r = \dfrac{4\, m_{inc}\, m_{tar}}{(m_{inc} + m_{tar})^2}$

Energy and momentum transfer can be shared by nucleus and electrons
→ Inelastic scattering
(energy loss in atomic energy level)
→ Phase space suppression

When atomic structures should be considered (free target approx. fail)?

- Incident momentum ~ 100 keV and below
  - The wavelengths of incident particles are about the same order with the size of the atom.
  - For Innermost orbital, the related momentum $\sim Z m_e \alpha \sim Z * 3$ keV (Z = effective nuclear charge)
- Energy transfer ~ 10 keV and below
  - barely overcome the atomic thresholds
  - For Innermost orbital, binding energy ~ 11 keV (Ge) and 34 keV (Xe)
- Phase-space suppression (Ex: WIMP-e scattering)

Scattering Diagrams

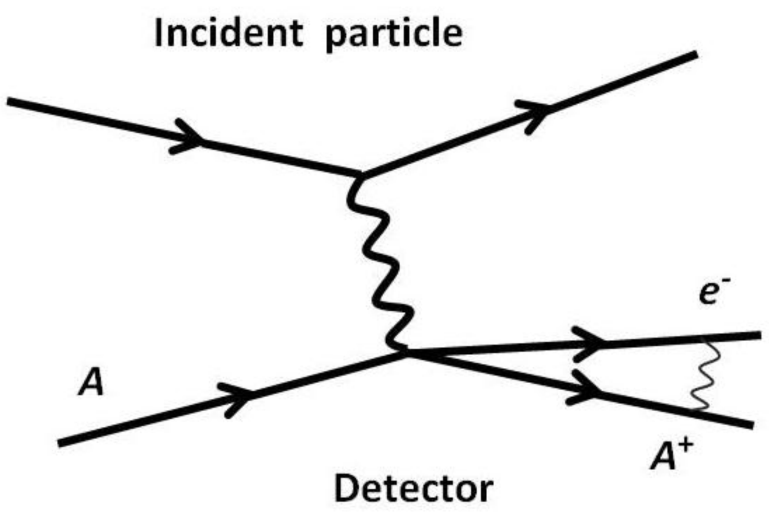

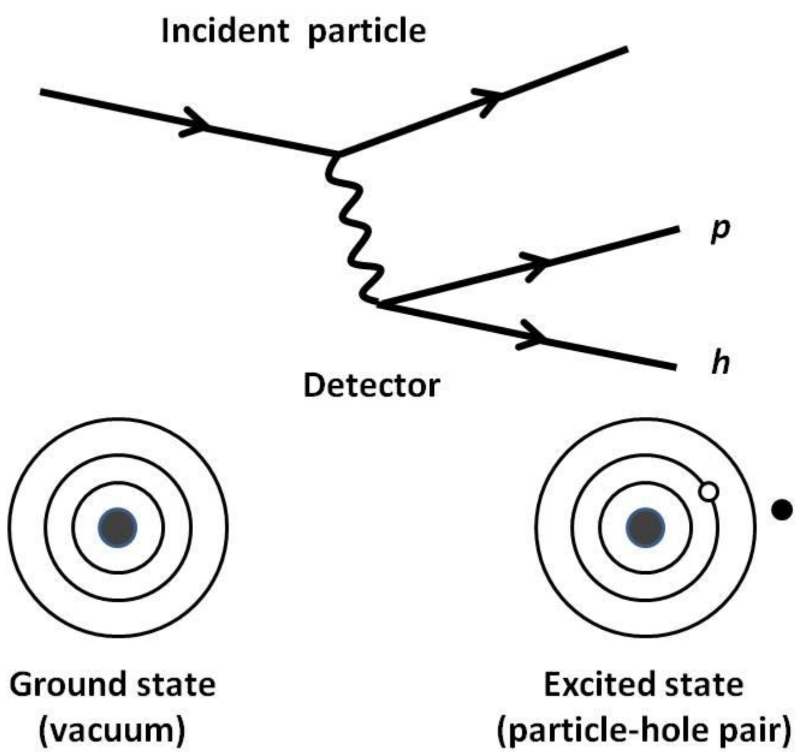

The atomic transition amplitudes can be calculated with the orbital wave functions of the atom.

Ab initio Theory for Atomic Ionization

MCDF: multiconfiguration Dirac-Fock method

Dirac-Fock method: $\psi(t)$ is a Slater determinant of one-electron orbitals $u_a(\vec{r},t)$ and invoke variational principle $\delta\left\langle \overline{\psi}(t) \right| i\frac{\partial}{\partial t} - H - V_I(t) \left| \psi(t) \right\rangle = 0$ to obtain eigenequations for $u_a(\vec{r},t)$.

multiconfiguration: Approximate the many-body wave function $\Psi(t)$
(for open shell atom) by a superposition of configuration functions $\psi_\alpha(t)$

$$\Psi(t) = \sum_\alpha C_\alpha(t)\,\psi_\alpha(t)$$

Ge: 2 e$^-$ in 4*p* (*j* = 1/2 or 3/2)

MCRRPA: multiconfiguration relativistic random phase approximation

RPA: Expand $u_a(\vec{r},t)$ into time-indep. orbitals in power of external potential

$$u_a(\vec{r},t) = e^{i\varepsilon_a t}\left[u_a(\vec{r}) + w_{a+}(\vec{r})e^{-i\omega t} + w_{a-}(\vec{r})e^{i\omega t} + \ldots \right]$$

$$C_a(t) = C_a + [C_a]_+ e^{-i\omega t} + [C_a]_- e^{i\omega t} + \ldots$$

Benchmark: Ge & Xe Photoionization

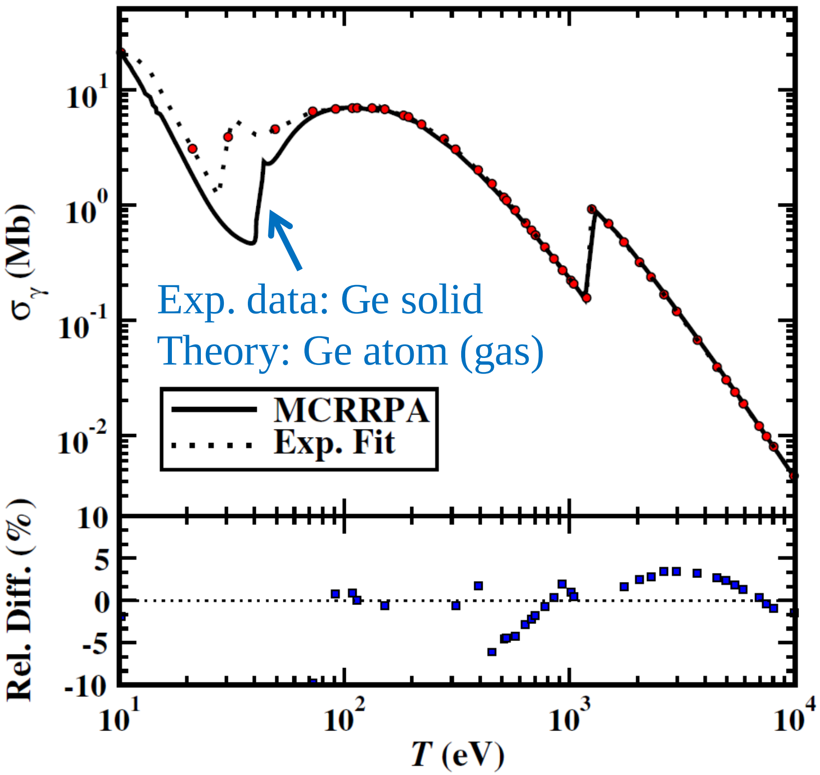

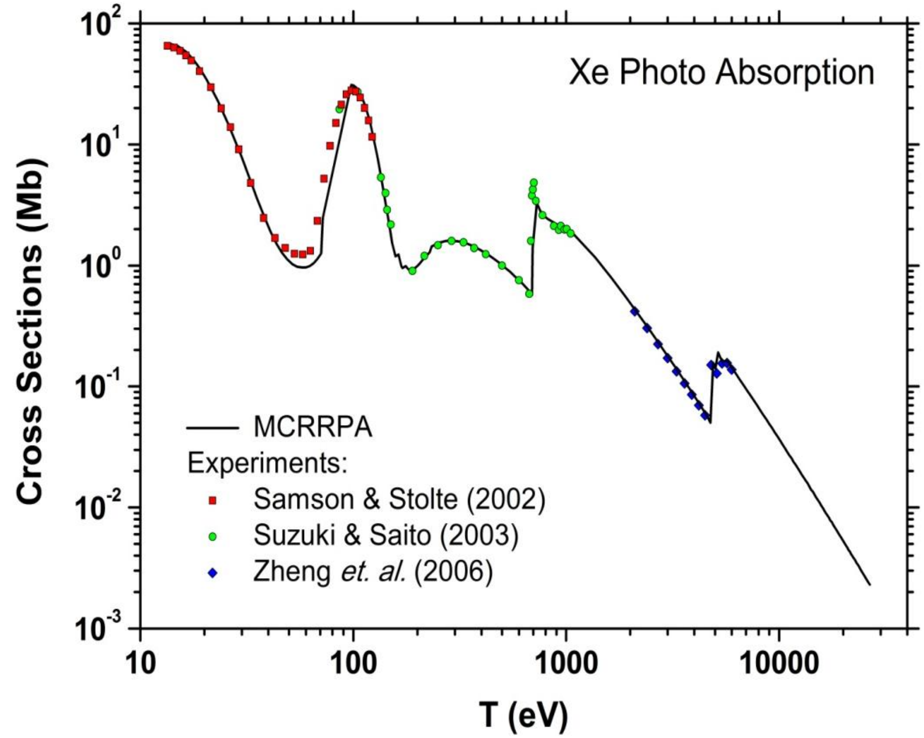

Above 100 eV error under 5%.

B. L. Henke, E. M. Gullikson, and J. C. Davis, Atomic Data and Nuclear Data Tables **54**, 181-342 (1993).
J. Samson and W. Stolte, J. Electron Spectrosc. Relat. Phenom. **123**, 265 (2002).
I. H. Suzuki and N. Saito, J. Electron Spectrosc. Relat. Phenom. **129**, 71 (2003).
L. Zheng *et al.*, J. Electron Spectrosc. Relat. Phenom. **152**, 143 (2006).

Interaction Channels of Neutrino-Induced Ge Ionization

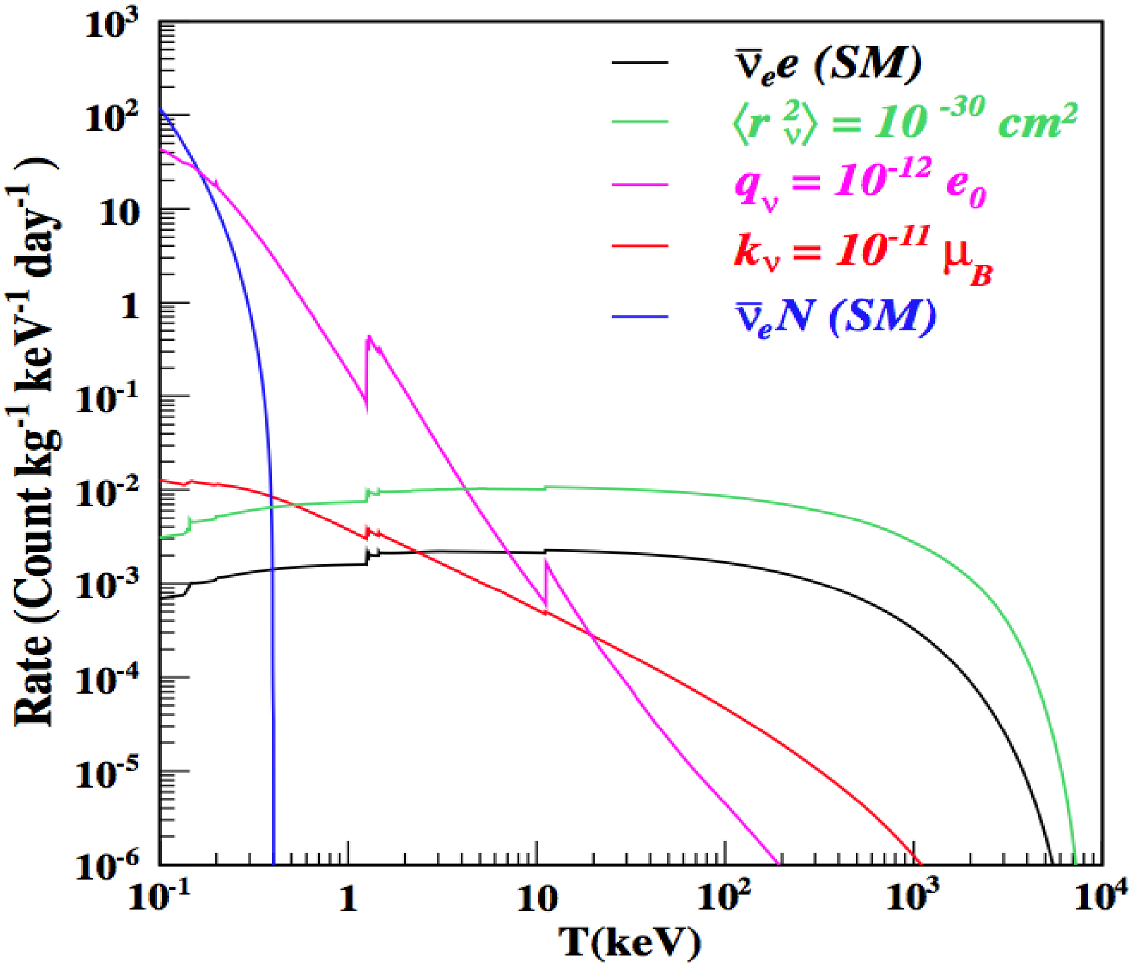

Applications I: Neutrino EM Properties

Data set	Reactor-$\bar{\nu}_e$ Flux ($\times 10^{13}$ cm^{-2} s^{-1})	Data strength Reactor on/off (kg-days)	Analysis Threshold (keV)	Bounds at 90% C.L. $\kappa_{\bar{\nu}_e}^{(\mathrm{eff})}$ ($\times 10^{-11} \mu_B$)	$\mathbb{q}_{\bar{\nu}_e}$ ($\times 10^{-12}$)	$\langle \mathbb{r}^2_{\bar{\nu}_e} \rangle^{(\mathrm{eff})}$ ($\times 10^{-30}$ cm^2)
TEXONO 187 kg CsI [9]	0.64	29882.0/7369.0	3000	< 22.0	< 170	< 0.033
TEXONO 1 kg Ge [5,6]	0.64	570.7/127.8	12	< 7.4	< 8.8	< 1.40
GEMMA 1.5 kg Ge [7,8]	2.7	1133.4/280.4	2.8	< 2.9	< 1.1	< 0.80
TEXONO point-contact Ge [4,17]	0.64	124.2/70.3	0.3	< 26.0	< 2.1	< 3.20
Projected point-contact Ge	2.7	800/200	0.1	< 1.7	< 0.06	< 0.74
Sensitivity at 1% of SM	...	...	...	~ 0.023	~ 0.0004	~ 0.0014

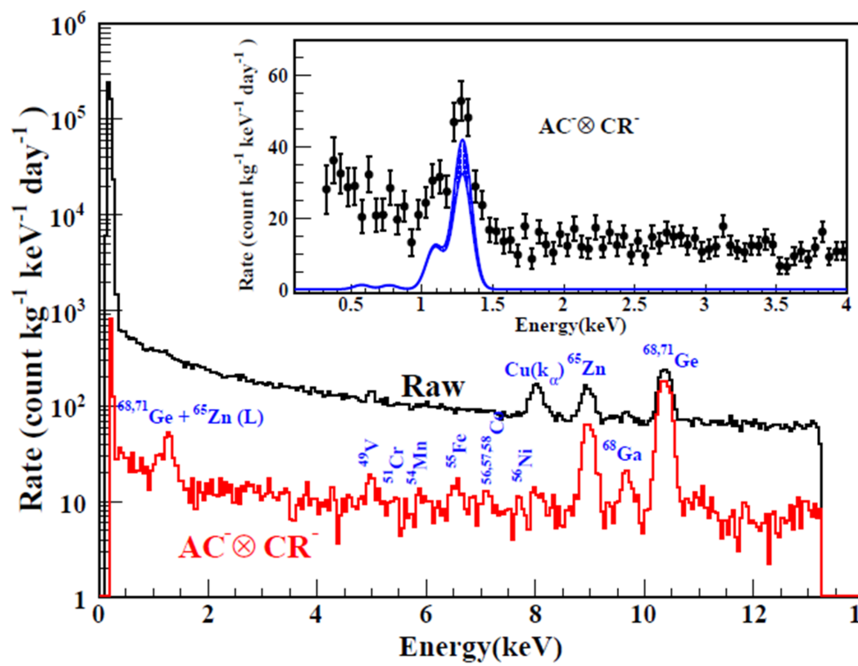

Reference:

Phys. Lett. B **731**, 159, arXiv:1311.5294 (2014).

Phys. Rev. D **90**, 011301(R), arXiv:1405.7168 (2014).

Phys. Rev. D **91**, 013005, arXiv:1411.0574 (2015).

Applications II: Solar ν Background in LXe Detectors

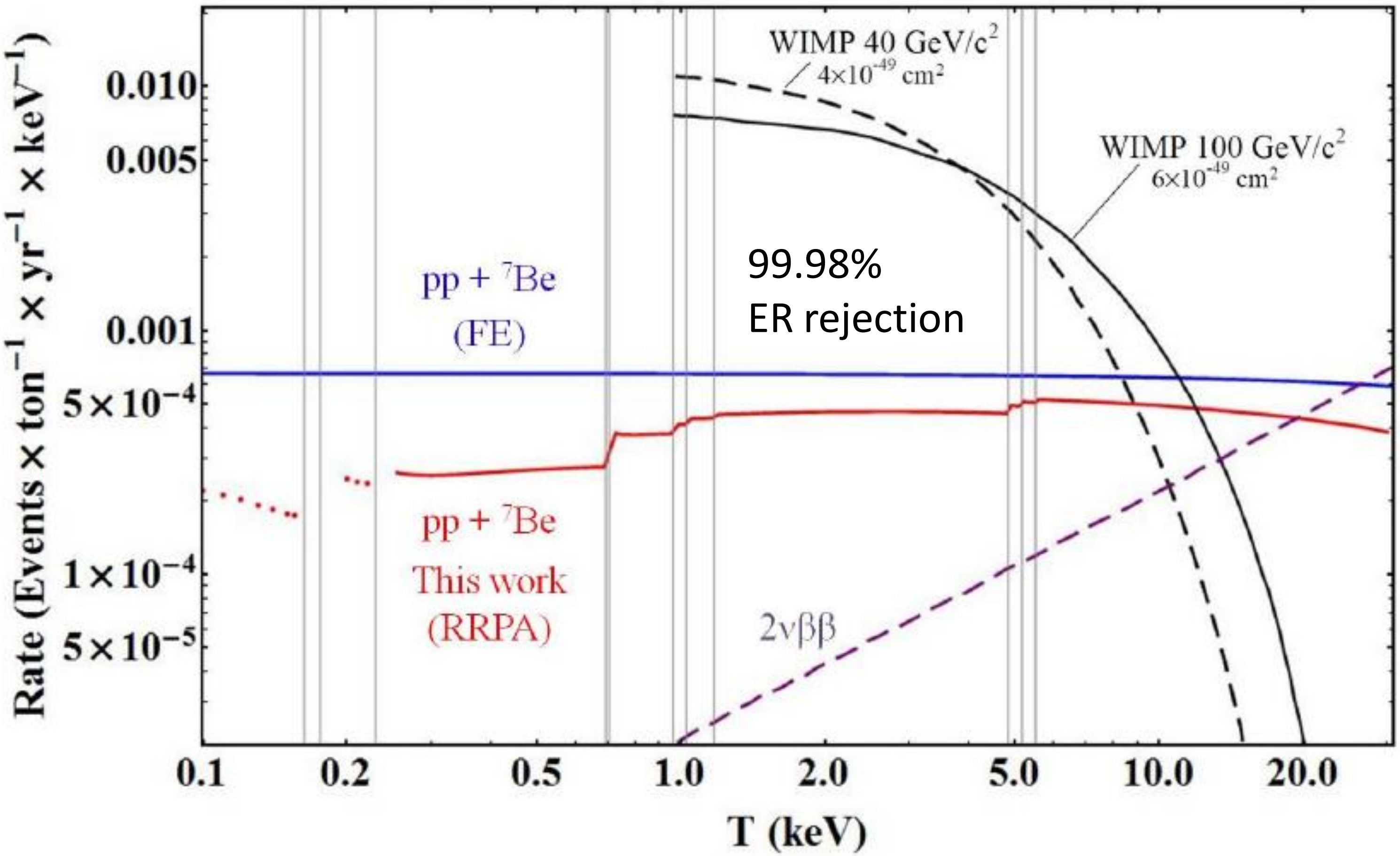

J. Aalbers *et. al.* (DARWIN collaboration), arXiv:1606.07001 (2016).
J.-W. Chen *et. al.*, arXiv:1610.04177 (2016).

Summary

- Benefits from low-threshold detectors, but atomic effects should be taken into consideration, because
  1. Energy and momentum transfers from neutrinos & LDM are around the atomic scale,
  2. Two-body free targets assumption is no longer an good estimation for the dominant kinematic region.
- *Ab initio* many-body calculations of Ge & Xe atomic ionization performed with ~5% estimated error. That can be applied for
  1. Constraining neutrino EM properties,
  2. Study on solar neutrino backgrounds in DM detection,
  3. Calculating DM atomic ionization cross sections.

Related Publications :

1. J.-W. Chen, H.-C. Chi, C.-P. Liu, and C.-P. Wu, arXiv:1610.04177.
2. J.-W. Chen, H.-C. Chi, S.-T. Lin, C.-P. Liu, L. Singh, H. T. Wong, C.-L. Wu, and C.-P. Wu, Phys. Rev. D **93**, 093012 (2016).
3. J.-W. Chen, H.-C. Chi, C.-P. Liu, C.-L. Wu and C.-P. Wu, Phys. Rev. D **92**, 096013 (2015).
4. J.-W. Chen, H.-C. Chi, K.-N. Huang, H.-B. Li, C.-P. Liu, L. Singh, H. T. Wong, C.-L. Wu, and C.-P. Wu, Phys. Rev. D **91**, 013005 (2015).
5. J.-W. Chen, H.-C. Chi, H.-B. Li, C.-P. Liu, L. Singh, H. T. Wong, C.-L. Wu, and C.-P. Wu, Phys. Rev. D **90**, 011301(R) (2014).
6. J.-W. Chen, H.-C. Chi, K.-N. Huang, C.-P. Liu, H.-T. Shiao, L. Singh, H. T. Wong, C.-L. Wu, and C.-P. Wu, Phys. Lett. B **731**, 159 (2014).
7. J.-W. Chen, C.-P. Liu, C.-F. Liu, and C.-L.Wu, Phys. Rev. D **88**, 033006 (2013).

Thanks for your attention!

Backup Slides

Neutrino: Atomic Ionization

$\nu + A \to \nu' + A^+ + e^-$

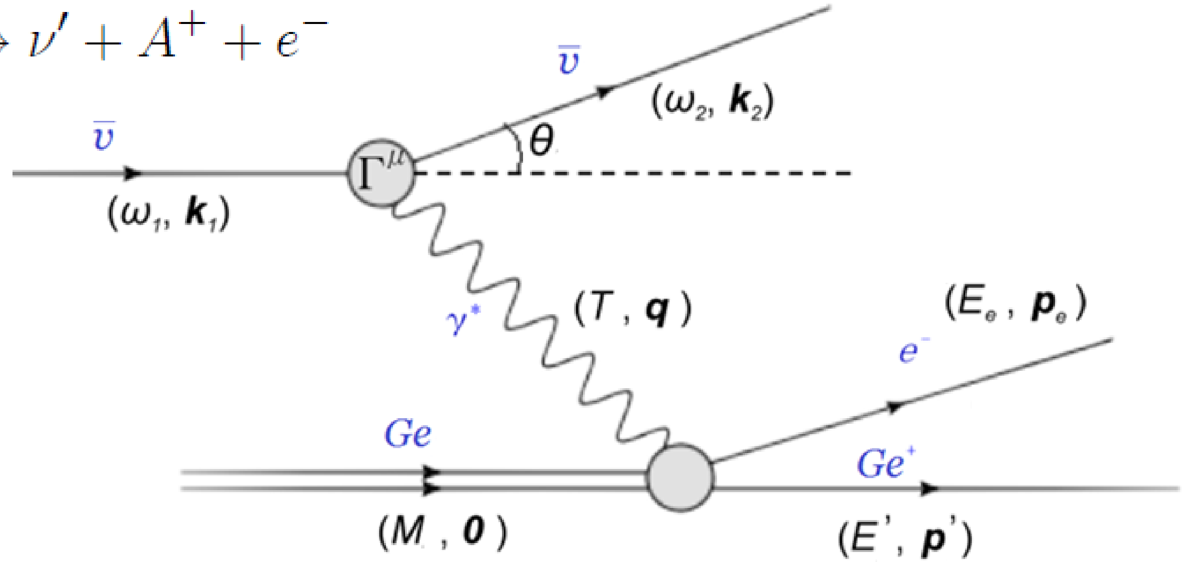

$$d\sigma = \frac{g^2}{\vec{v}_1} \frac{\bar{l}^{\mu\nu}\, \bar{W}_{\mu\nu}}{(q^2 - m_b^2)^2} (2\pi)^4\, \delta^4(k_1 + p_A - k_2 - p_R - p_r) \frac{d^3\vec{k}_2}{(2\pi)^3} \frac{d^3\vec{p}_R}{(2\pi)^3} \frac{d^3\vec{p}_r}{(2\pi)^3}$$

Leptonic tensor: $\bar{l}^{\mu\nu} \equiv \sum_{s_2} \overline{\sum_{s_1}} \langle k_2, s_2 | j_l^\mu | k_1, s_1 \rangle \, \langle k_2, s_2 | j_l^\nu | k_1, s_1 \rangle^*$

Atomic tensor: $\overline{W}^{\mu\nu} \equiv \sum_{m_{j_f}} \overline{\sum_{m_{j_i}}} \langle f | j_A^\mu | i \rangle \, \langle f | j_A^\nu | i \rangle^*$

Leptonic Tensor Part

$$\bar{l}^{\mu\nu} \equiv \sum_{s_2} \overline{\sum_{s_1}} \langle k_2, s_2 | j_l^{\mu} | k_1, s_1 \rangle \, \langle k_2, s_2 | j_l^{\nu} | k_1, s_1 \rangle^*$$

$$\langle k_2 | \hat{j}_l^{\mu} | k_1 \rangle = j_\mu^{(w)} + j_\mu^{(\gamma)}$$

w: The neutrino weak current

γ: The electromagnetic current

$$j_\mu^{(w)} = \bar{\nu}(k_2, s_2)\gamma_\mu(1-\gamma_5)\nu(k_1, s_1)$$

$$j_\mu^{(\gamma)} = \bar{\nu}(k_2, s_2)[F_1(q^2)\gamma_\mu - i(F_2(q^2) + iF_E(q^2)\gamma_5)\sigma_{\mu\nu}q^\nu + F_A(q^2)(q^2\gamma_\mu - \not{q}q_\mu)\gamma_5]\nu(k_1, s_1)$$

The Form Factors & Related Physical Quantities

$F_1(q^2)$: charge form factor

$F_2(q^2)$: anomalous magnetic

$F_A(q^2)$: anapole (*P*-violating)

$F_E(q^2)$: electric dipole

(*P*, *T*-violating)

neutrino millicharge :

$$\mathbb{q}_\nu = F_1(0),$$

charge radius squared :

$$\langle \mathbb{r}_\nu^2 \rangle = 6 \frac{d}{dq^2} F_1(q^2) \Big|_{q^2 \to 0}$$

neutrino magnetic moment :

$$\kappa_\nu = F_2(0),$$

anapole moment :

$$\mathbb{a}_\nu = F_A(0),$$

electric dipole moment :

$$\mathbb{d}_\nu = F_E(0),$$

Atomic Tensor Part

$$\overline{W}^{\mu\nu} \equiv \sum_{m_{j_f}} \overline{\sum_{m_{j_i}}} \langle f|j^\mu_A|i\rangle \, \langle f|j^\nu_A|i\rangle^*$$

$$\langle f^{(-)}|j^\mu_A|i\rangle = c_V \mathcal{J}^\mu - c_A \mathcal{J}^\mu_5$$

$$c_V = -\frac{1}{2} + 2\sin^2\theta_w + \delta_{l,e}$$

$$c_A = -\frac{1}{2} + \delta_{l,e}$$

The atomic (axial-)vector current:

$$\mathcal{J}^\mu_{(5)} \equiv \langle \Psi_f | \hat{\mathcal{J}}^\mu_{(5)}(-\vec{q}) | \Psi_i \rangle$$

$$= \int d^3x e^{i\vec{q}\cdot\vec{x}} \langle \Psi^{(-)}_f | \hat{\bar{\psi}}_e(\vec{x}) \gamma^\mu (\gamma_5) \hat{\psi}_e(\vec{x}) | \Psi_i \rangle$$

Scattering Amplitude

The weak scattering amplitude:

$$\mathcal{M}^{(w)} = \frac{G_F}{\sqrt{2}} j_\mu^{(w)} (c_V \mathcal{J}^\mu - c_A \mathcal{J}_5^\mu)$$

The EM scattering amplitude:

$$\mathcal{M}^{(\gamma)} = \frac{4\pi\alpha}{q^2} j_\mu^{(\gamma)} \mathcal{J}^\mu$$

Neutrino-Impact Ionization Cross Sections

neutrino weak scattering :

$$\frac{d\sigma_w}{dT} = \frac{G_F^2}{2\pi^2}(E_\nu - T)^2 \int \cos^2\frac{\theta}{2}\Big\{R_{00} - \frac{T}{|\vec{q}|}R_{03+30} + \frac{T^2}{|\vec{q}|^2}R_{33} + \left(\tan^2\frac{\theta}{2} + \frac{|\vec{q}|^2}{2\,q^2}\right)R_{11+22} + \tan\frac{\theta}{2}\sqrt{\tan^2\frac{\theta}{2} + \frac{|\vec{q}|^2}{q^2}}R_{12+21}\Big\}d\Omega_{\mathbf{k}_2}$$

neutrino magnetic moment scattering :

$$\frac{d\sigma_\mu}{dT} = \left(\frac{\alpha F_2}{2m_e}\right)^2\left(1 - \frac{T}{E_\nu}\right)\int\Big\{-\frac{(2E_\nu - T)^2 q^2}{q^4}R_{00} + \frac{q^2 + 4E_\nu(E_\nu - T)}{2|\vec{q}|^2}R_{11+22}\Big\}d\Omega_{\mathbf{k}_2}$$

neutrino millicharge scattering:

$$\frac{d\sigma_C}{dT} = F_1^2\left(\frac{E_\nu - T}{E_\nu}\right)\int\Big\{\frac{(2E_\nu - T)^2 - |\vec{q}|^2}{q^4}R_{00} - \left[\frac{q^2 + 4E_\nu(E_\nu - T)}{2q^4} + \frac{1}{q^2}\right]R_{11+22}\Big\}d\Omega_{\mathbf{k}_2}$$

Atomic Response Functions

$$R^{(w)}_{\mu\nu} = \frac{1}{2J_i+1}\sum_{M_{J_i}}\sum_{f}\langle\Psi^{(-)}_f|c_V\hat{\mathcal{J}}_\mu - c_A\hat{\mathcal{J}}_{5\mu}|\Psi_i\rangle \times \langle\Psi_f|c_V\hat{\mathcal{J}}_\nu - c_A\hat{\mathcal{J}}_{5\nu}|\Psi_i\rangle^*\delta(T+E_i-E_f)$$

Do multipole expansion with J

Final continuous wave functions could be obtained by **MCRRPA** and expanded in the (J, L) basis of orbital wave functions

Initial states could be approximated by bound electron orbital wave functions given by **MCDF**

$$R^{(w)}_{\mu\nu}\big|_{c_V=1,c_A=0} \rightarrow R^{(\gamma)}_{\mu\nu}$$

The Transition Amplitude

$$\langle \Psi_f^{(-)} | v_+ | \Psi_i \rangle = \sum_\alpha \Lambda_\alpha (\langle w_{\alpha+} | v_+ | u_\alpha \rangle + \langle u_\alpha | v_+ | w_{\alpha-} \rangle)$$
$$+ \sum_{a,b} ([C_a]_+^\star C_b + C_a^\star [C_b]_-) \langle \psi_a | v_+ | \psi_b \rangle$$

The single-electron perturbing field:

$$v_+ = \int d^3x \;\; e^{i\vec{q}\cdot\vec{x}} \;\, l_\mu(\vec{x}) \, \hat{J}^\mu(\vec{x}) \, , \qquad v_- = v_+^\dagger$$

$$\mathbf{l} = \sum_{\lambda=0,\pm1} l_\lambda \, \hat{e}_\lambda^\dagger$$

$\hat{e}$: basis a set of polarization vectors

$$\hat{e}_{(\lambda=\pm1)} \; e^{i\vec{q}\cdot\vec{x}} = \sum_{J\geq1} i^J \sqrt{2\pi(2J+1)} \left\{ \mp j_J(kr) \mathcal{Y}_{JJ1}^\lambda - \frac{1}{k} \nabla \times \left[j_J(kr) \mathcal{Y}_{JJ1}^\lambda \right] \right\}$$

$$\hat{e}_{(\lambda=0)} \; e^{i\vec{q}\cdot\vec{x}} = \frac{-i}{k} \sum_{J\geq0} i^J \sqrt{4\pi(2J+1)} \, \nabla \left[j_J(kr) \, Y_{J0} \right]$$

Multipole Expansion & Operators

$$\hat{C}_{JM}(k) = \int d^3x [j_J(kr) Y_{JM}] \, \hat{J}_0(\vec{x})$$

$$\hat{L}_{JM}(k) = \frac{i}{k} \int d^3x \{\nabla[j_J(kr) Y_{JM}]\} \cdot \hat{J}(\vec{x})$$

$$\hat{E}_{JM}(k) = \frac{1}{k} \int d^3x \, [\nabla \times j_J(kr) \mathcal{Y}^M_{JJ1}] \cdot \hat{J}(\vec{x})$$

$$\hat{M}_{JM}(k) = \int d^3x [j_J(kr) \mathcal{Y}^M_{JJ1}] \cdot \hat{J}(\vec{x})$$

The EM perturbing field can be expressed as

$$v_+^{(\gamma)} = \frac{4\pi\alpha}{q^2} \Big\{ \sum_{J=0}^{\infty} \sqrt{4\pi(2J+1)} \, i^J [j_0^{(\gamma)} \hat{C}_{J0}(k) - j_3^{(\gamma)} \hat{L}_{J0}(k)] + \sum_{J\geq 1}^{\infty} \sqrt{2\pi(2J+1)} \, i^J \sum_{\lambda=\pm 1} j_\lambda^{(\gamma)} [\hat{E}_{J-\lambda}(k) - \lambda \hat{M}_{J-\lambda}(k)] \Big\}$$

Approximation Schemes

Longitudinal Photon Approx. (LPA) : $V_T = 0$

Equivalent Photon Approx. (EPA) : $V_L = 0,\ q^2 = 0$

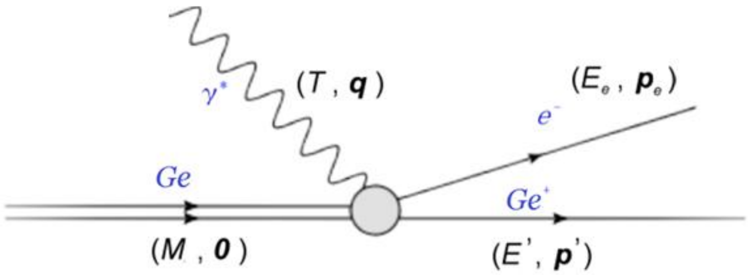

① Strong q^2-dependence in the denominator : long-range interaction

② Real photon limit $q^2 \sim 0$: relativistic beam or soft photons $q^\mu \sim 0$

Free Electron Approx. (FEA) : $q^2 = -2\, m_e T$

$$\left.\frac{d\sigma}{dT}\right|_{\mathrm{FEA}} = \sum_{i=1}^{Z} \theta(T - B_i) \left.\frac{d\sigma^{(0)}}{dT}\right|_{q^2=-2m_e T}$$

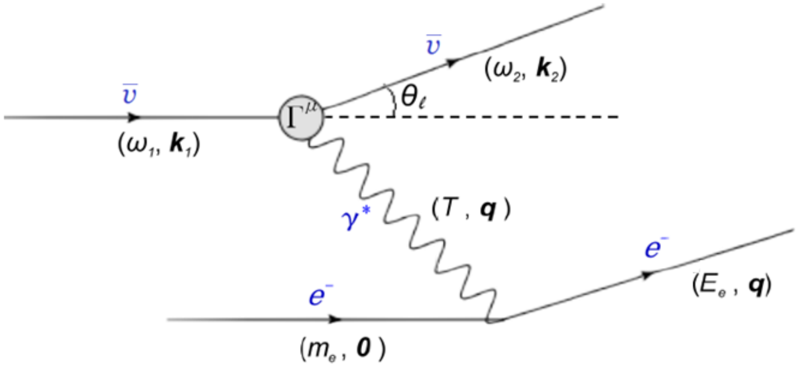

① Main contribution comes from the phase space region similar with 2-body scattering

② Atomic effects can be negligible :
$E_\nu >> Z m_e \alpha$
$T \neq B_i$ (binding energy)

Toy Model: NMM with *H* target (analytic result obtained)

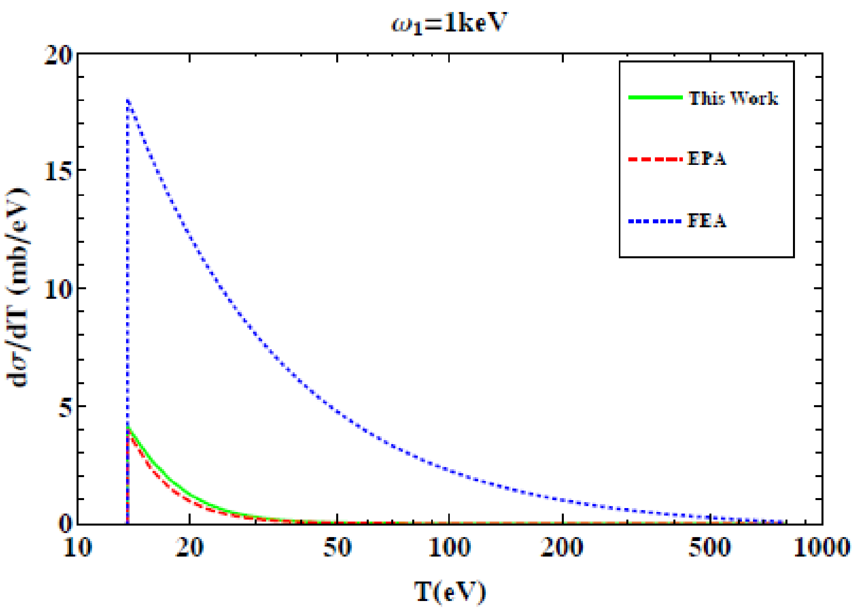

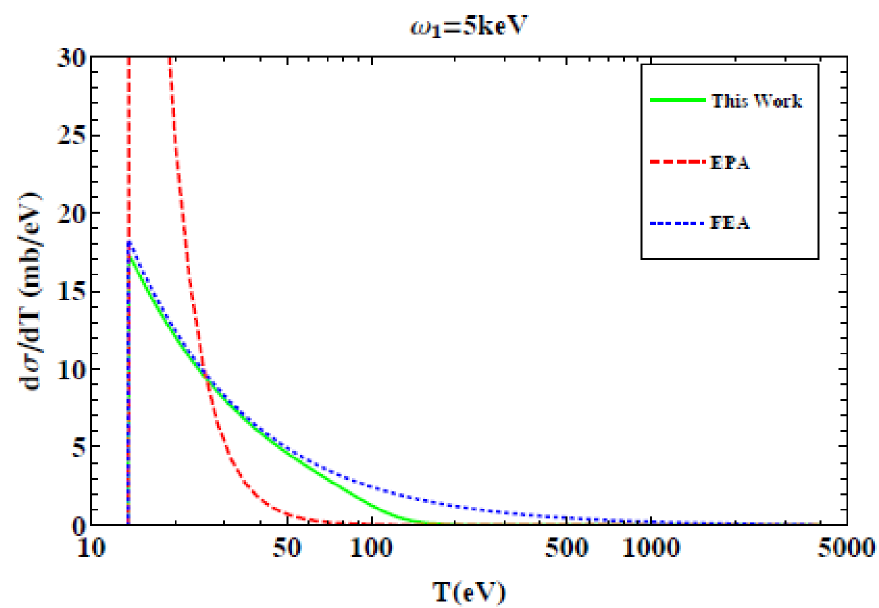

Equivalent Photon Approx.

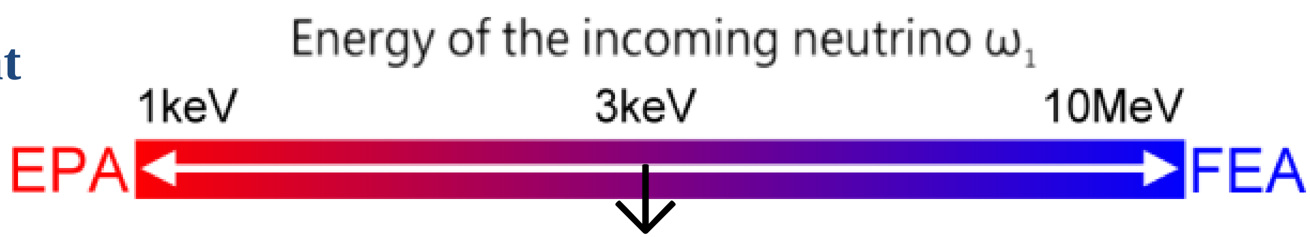

Free Electron Approx.

binding momentum of hydrogen: $m_e\alpha$

J.-W. Chen, C.-P. Liu, C.-F. Liu, and C.-L. Wu, Phys. Rev. D **88**, 033006 (2013).

Numerical Results: Weak Interaction

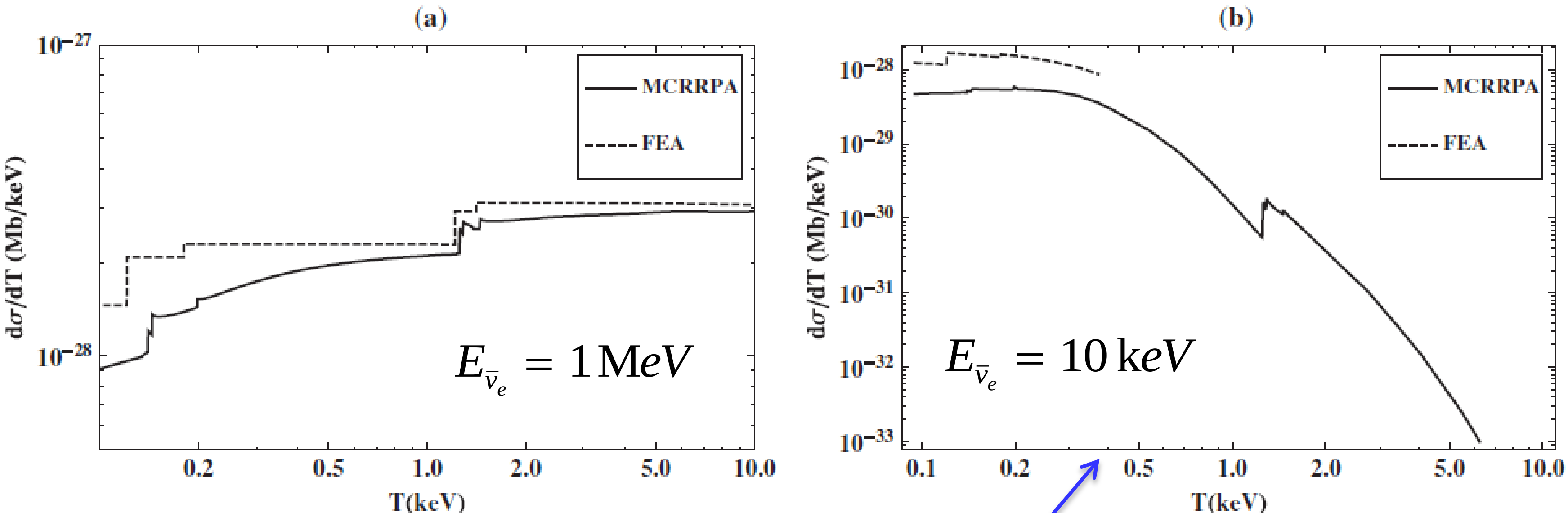

(1) short range interaction
(2) neutrino mass is tiny
(3) $E_\nu >> Z m_e \alpha$

FEA works well away from the ionization thresholds.

$$\text{cutoff}: T_{\text{Max}} = \frac{2E_{\bar{\nu}_e}^2}{2E_{\bar{\nu}_e} + m_e} \approx 0.38\,\text{keV}$$

$$\vec{p}_r \approx \sqrt{2m_e T} \le \vec{q}_{Max} \approx 2E_{\bar{\nu}_e} - T$$

(backward scattering, $m_{\bar{\nu}_e} \to 0$)

Numerical Results: NMM

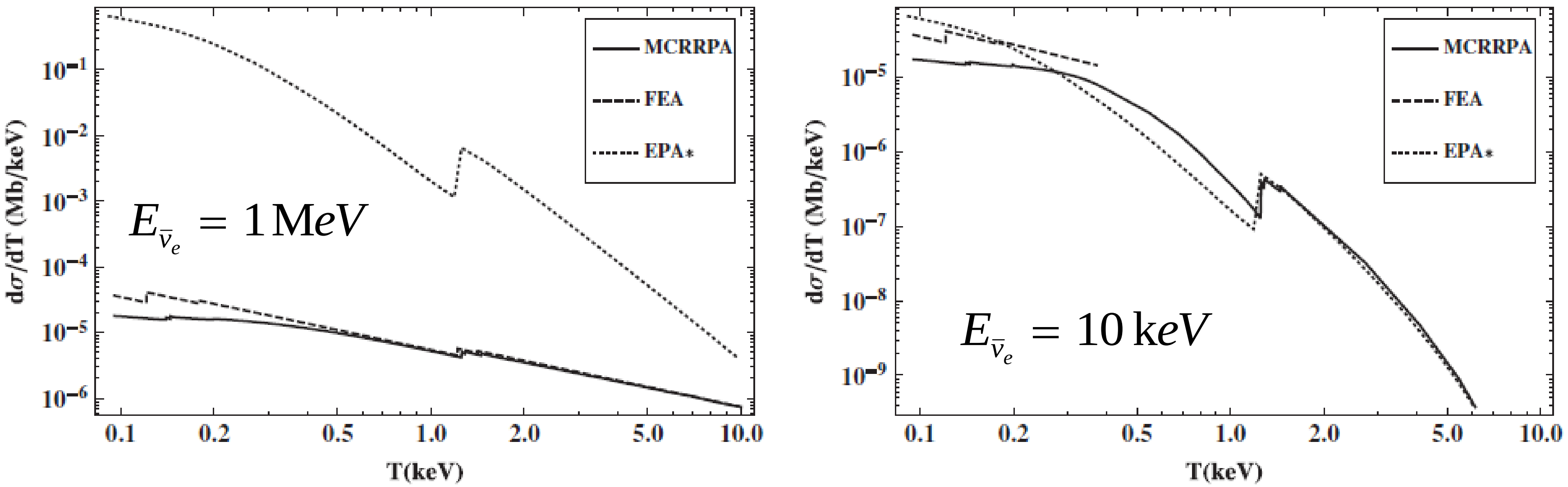

Similar with WI cases. FEA still faces a cutoff with lower E_ν .

For right plot, EPA becomes better when T approaches to E_ν (q^2 -> 0).

Consistent with Hydrogen results.

Numerical Results: Millicharge

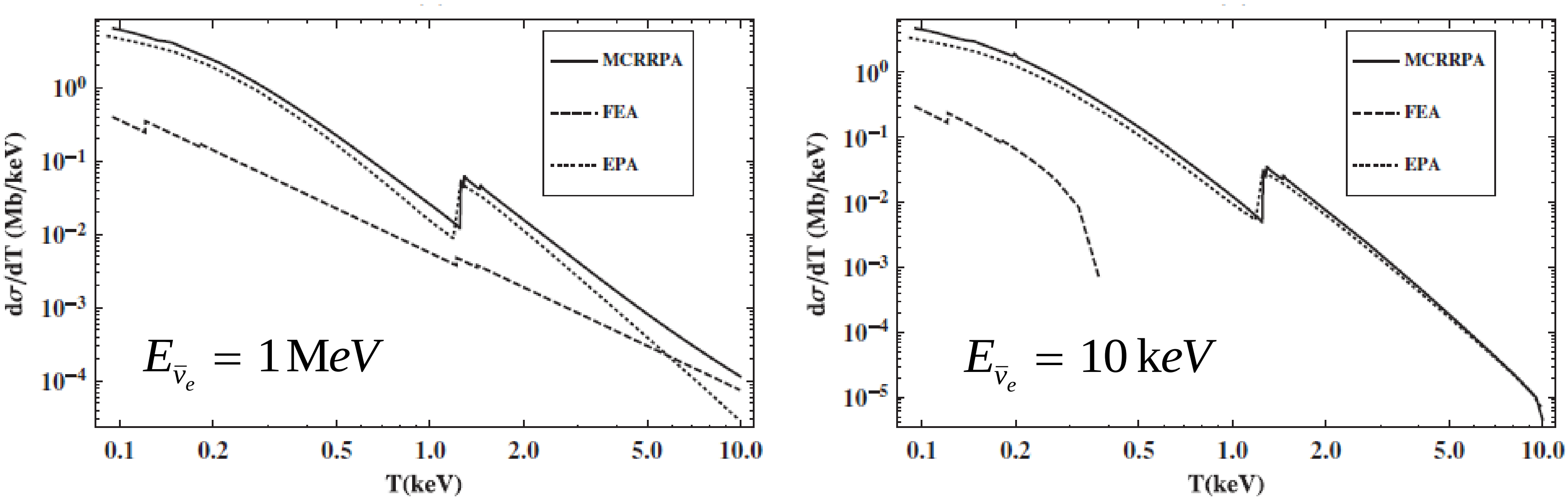

EPA worked well due to q^2 dependence in the denominator of scattering formulas of F_1 form factor (a strong weight at small scattering angles).

Applications III: Sterile Neutrino Direct Detection

ν_s **: massive, non-relativistic**

$\omega_1 \sim m_s$

$\boldsymbol{k_1 << k_2}$

ν_a **: almost massless, relativistic**

$\omega_2 \sim \boldsymbol{k_2} \sim \boldsymbol{q}$

$\omega_2 = \omega_1 - T$

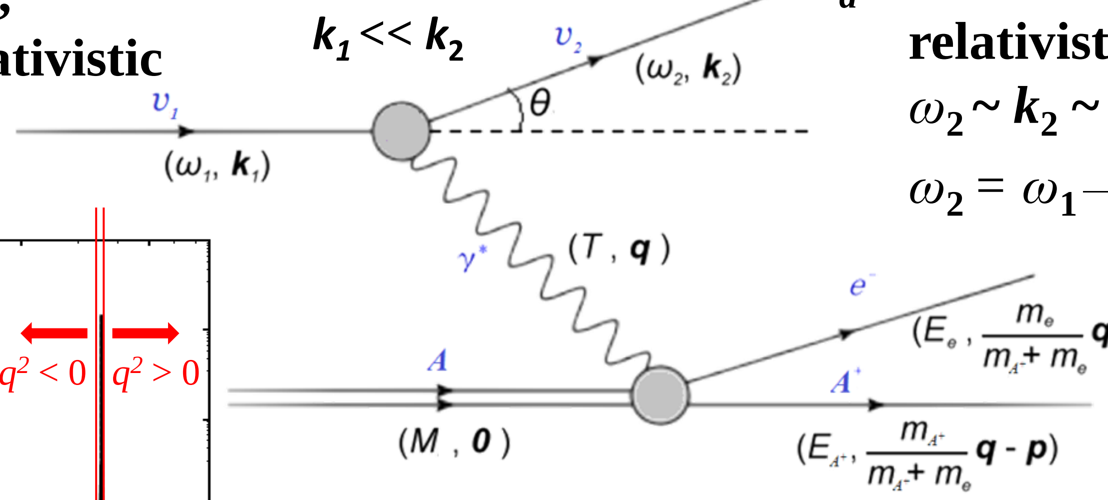

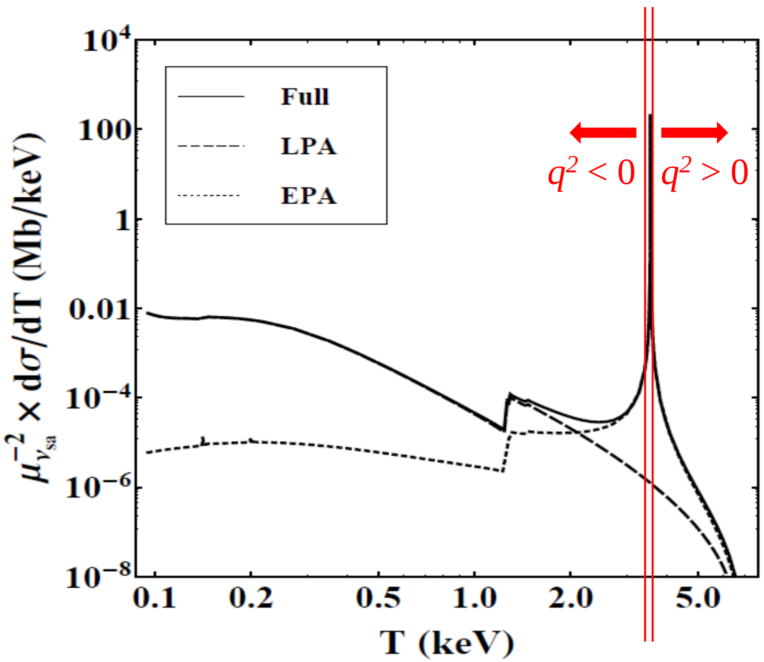

(a) $m_s = 7.1\,\mathrm{keV}$

$$\nu_s + \mathrm{A} \rightarrow \nu_a + \mathrm{A}^+ + e^-$$

$q^2 > 0$ at forward scattering when $T > \omega_1/2$

$$\nu_a + \mathrm{A} \rightarrow \nu_a + \mathrm{A}^+ + e^-$$

$q^2 < 0$ for all possible scattering angle & T

J.-W. Chen *et al.*, Phys. Rev. D **93**, 093012, arXiv:1601.07257 (2016).

Constraints by TEXONO data

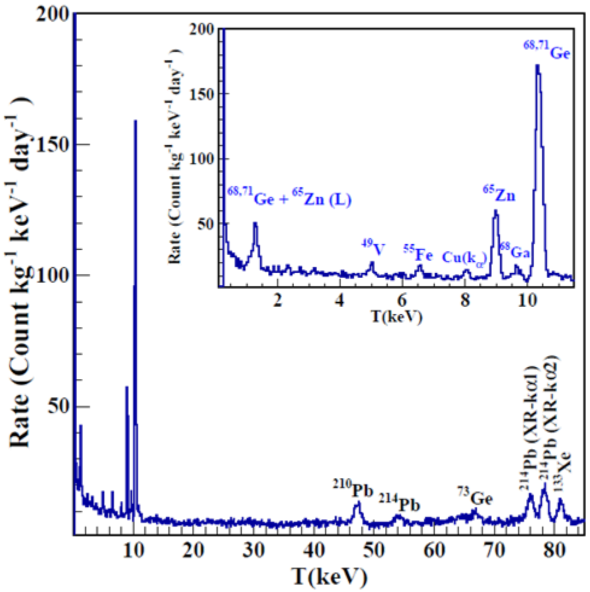

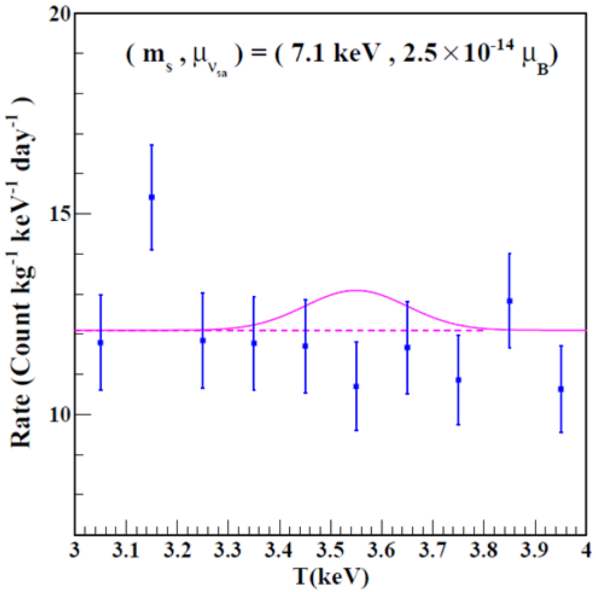

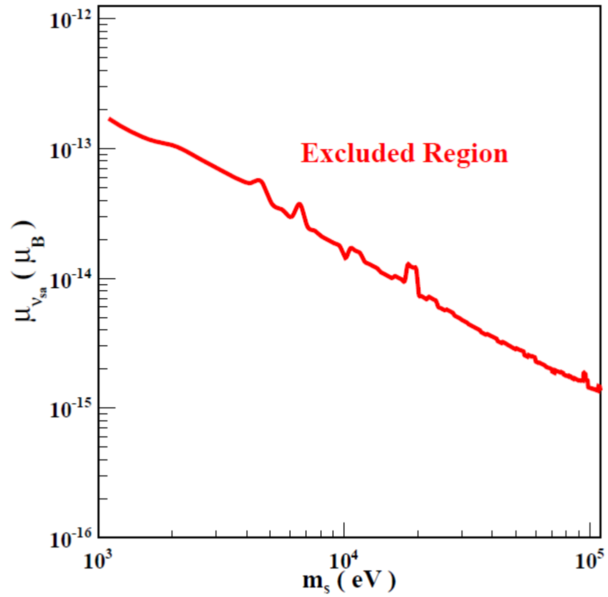

$$\left(\frac{dR}{dT}\right) = \frac{\rho_s}{m_A m_s}\int_0^{v_{\max}} \frac{d\sigma(m_s, v)}{dT} v f(\vec{v}) d^3 v$$

Maxwellian velocity distribution

$$f(\vec{v}) = N_0 e^{(-\vec{v}^2/v_0^2)}\Theta\left(v_{\rm esc} - |\vec{v}|\right)$$

- At m_s = 7.1 keV, the upper limit of $\mu_{\nu sa} < 2.5*10^{-14}\ \mu_B$ at 90% C.L.
- The recent X-ray observations of a 7.1 keV sterile neutrino with decay lifetime $1.74*10^{-28}\ s^{-1}$ can be converted to $\mu_{\nu sa} = 2.9*10^{-21}\ \mu_B$, much tighter because its much larger collecting volume.

Applications IV: DM Scattering